

Magnetic and electronic properties of Ni films, surfaces, and interfaces

J. Tersoff* and L. M. Falicov

*Materials and Molecular Research Division, Lawrence Berkeley Laboratory, Berkeley, California 94720
and Department of Physics, University of California, Berkeley, California 94720*

(Received 17 June 1982)

Results of various calculations lead to a unified understanding of the magnetic behavior of thin nickel films. We thus explain disparate experimental results. We report results for magnetic and electronic properties of Ni films of one to five atomic layers on Cu (100) and (111), of the Ni-Cu (100) and (111) interfaces, and of the Ni (100) and (111) surfaces. Results are in good agreement with the few published calculations. We find that magnetization is suppressed at the Ni-Cu interface, but enhanced in isolated thin films. The net effect of this competition is that a Ni monolayer is substantially magnetic on Cu(100) but paramagnetic (or nearly so) on Cu(111). Film magnetization is found to be very sensitive to substrate composition. For substrates which couple strongly to the Ni film, ferromagnetism first appears at about three atomic layer Ni, in quantitative agreement with experiments based on Al and Pb-Bi substrates. The crucial mechanism acting to suppress Ni magnetization is *sp-d* hybridization, just as in most Ni alloys.

I. INTRODUCTION

Recent studies¹⁻⁵ of the magnetic behavior of thin films have yielded disparate and apparently contradictory results. In particular, the question of the presence or absence of magnetically "dead" (i.e., paramagnetic) layers of Ni or Fe has attracted attention and generated some controversy. Despite the increasing care and sophistication of recent work, a consistent picture of the magnetic behavior of ultrathin films remains elusive.

A major factor contributing to the confused situation is, we believe, the absence of a simple, coherent theoretical perspective from which to view the experimental results. Nickel is an itinerant ferromagnet; that is, its magnetization derives from the spin polarization of the itinerant *d* electrons. These *d* electrons are very sensitive to local environment, and so the magnetic properties become intertwined with the electronic structure in a complex manner. In the simplest case, that of a pure infinite crystal, the simple rigid-band model of Stoner⁶ gives a reasonable account of itinerant ferromagnetism at $T=0$. For inhomogeneous systems, however, the picture is far from clear. For surfaces and, *a fortiori*, thin films, while some theoretical calculations have been reported,⁷⁻¹¹ these have been too limited in scope to form the basis for a unified understanding of surface and film magnetism.

Our primary aim in this paper is to gain insight into the mechanisms determining the magnetic behavior of films, surfaces, and interfaces. We

choose Ni-Cu systems for theoretical investigation. These metals have very similar properties, and so form ideal substitutional alloys and epitaxial films with minimal charge transfer. While the calculations we present are mostly for Ni and Ni-Cu systems, the understanding gained permits us to draw conclusions about other systems too.

From the calculations reported here, together with available experimental results, a coherent picture of the important factors determining local magnetization in these inhomogeneous systems emerges. We thus place most of the disparate experiment results in a satisfying, consistent perspective.

It is not yet feasible to carry out such an extensive program of calculations using the most sophisticated computational tools currently available. Fully self-consistent methods are so numerically intensive that only a few simple ferromagnetic surfaces,⁷⁻⁹ and only one film system,¹⁰ have been studied to date. Our results are in excellent overall agreement with these state-of-the-art calculations. At the same time, the simpler methods used here permit a convenient, unified treatment of a relatively wide range of systems. By such a unified handling of surfaces, interfaces, and films, we develop the experience to draw simple generalizations about the dominant physical effects.

The remainder of this section is divided into three parts. Section IA gives background on the available experimental results for films, surfaces, and interfaces; Sec. IB gives theoretical back-

ground, in particular a discussion about the best available calculations for such systems; Sec. I C summarizes the scope of this paper and our results. Section II of this paper presents details of the calculation, Sec. III discusses our results, and the conclusions are set forth in Sec. IV.

A. Experimental background

Over a decade ago Liebermann *et al.*¹ sparked interest in film magnetism by reporting the observation of magnetically "dead" (i.e., paramagnetic) layers in thin Ni films on a Cu substrate. They interpreted this as a surface effect, supposing that a few layers at the surface of Fe or Ni are magnetically dead, so that for sufficiently thin films only these dead surface layers remain. This interpretation, while physically plausible, is almost certainly incorrect, and has had the unfortunate effect of distracting attention from the crucial role of the substrate.

More recent experiments have directly probed the magnetization of a Ni surface using photoemission,¹² electron-capture spectroscopy (ECS),^{2,13} and spin-polarized low-energy electron diffraction.¹⁴ While none of these methods provides a quantitative determination of the surface magnetization, all experiments agree that the surface layer of Ni is magnetic.

Results for thin Ni films are more complex and, on their face, inconsistent. Liebermann *et al.*¹ generated their thin films by electroplating, rather than by clean ultrahigh-vacuum methods as in more recent work. The possibility that they were observing some effect of surface oxidation or hydrogenation cannot therefore be ruled out. Later careful experiments with thin Ni films on Cu substrates^{2,3} have failed to find any evidence of magnetically dead layers. We note, however, that none of these experiments has examined Ni films of less than two atomic layers. Rau,¹² by means of ECS, found that a two-layer Ni film was definitely magnetic. Pierce and Siegmann³ found similar results using spin-polarized photoemission. While they extrapolate their results to thinner films, the extrapolation assumes a fixed number of dead layers independent of film thickness; we find that such an assumption is unwarranted and probably incorrect, as discussed later in this paper.

On the other hand, experiments by Bergmann⁴ and Meservey *et al.*⁵ clearly show a transition from ferromagnetism to paramagnetism as Ni film thickness is reduced below 2.5–3 atomic layers. These

experiments were carried out using a Pb-Bi alloy substrate and an Al substrate, respectively. We demonstrate below that the magnetic behavior of the Ni film may be expected to depend sensitively on substrate composition, in agreement with the available data.

Bergmann⁴ and Meservey *et al.*⁵ also found that Fe retained its magnetic moment down to submonolayer film thickness, even on the substrates where Ni lost its moment at 2.5–3 atomic layers. This too is consistent with our results, though it is not surprising in any case.

It is unfortunate that, to date, no one has systematically studied the dependence of Ni films magnetization on substrate composition (though a related experiment by Gradmann¹⁵ is very suggestive); nor has the study of Ni films on Cu been carried to monolayer and submonolayer coverage. Nevertheless, the available experimental information, together with the results presented below, form a compelling picture regarding the role of film thickness and substrate composition in determining film magnetization.

B. Theoretical background

In the brief history of fully self-consistent calculations of surface magnetism, no system has been more widely studied than the ideal Ni(100) surface. In fact, few other systems have been studied at all. Wang and Freeman¹⁷ reported a substantial decrease (about 25%) in the surface magnetization, relative to the bulk value. That calculation used a nine-layer film to mimic the semi-infinite crystal. On the other hand, results of Jepsen *et al.*⁸ and Krakauer and Freeman⁹ suggest a small enhancement in the surface magnetism; a quantitative value is, however, difficult to extract because of the thin five-layer films used.

The apparent discrepancy among reported calculations is somewhat worrisome, but may be attributable simply to aspects of the numerical implementation in early work. A more fundamental problem is the difficulty in finding relevant comparisons to experiment, in order to gauge the true accuracy of any theoretical results. For now, the quantitative reliability of *any* theoretical treatment of surface magnetism remains an open question.

Wang and Freeman have also reported¹⁶ a substantial enhancement (~50%) of the surface magnetism of Fe(100) relative to the bulk, and Noffke and Fritsche¹¹ and Wang *et al.*¹⁰ find that (hypothetical) monolayer films of Ni and Fe, with

vacuum on both sides, have magnetizations substantially greater than the metallic bulk values (though still smaller than the respective atomic spin values). These results clearly controvert the suggestion¹ of magnetically dead surface layers. They suggest, on the contrary, that surfaces and especially thin films tend to have *enhanced* magnetization. This tendency is moreover consistent with the naive argument that reduced coordination number will lead to band narrowing and a larger density of states (DOS) at the Fermi level (E_F), and hence to stronger magnetization. We argue that it is the interaction with a nonmagnetic substrate which overwhelms this tendency and suppresses the film magnetization in experiments on supported Ni films.

Only one calculation has been reported for the magnetization of a supported film. Wang *et al.*¹⁰ find that a monolayer Ni film on Cu(100) is substantially magnetic, with a magnetic moment per Ni atom which is reduced about 40% from the bulk value. That calculation employed one of the most advanced techniques now available; unfortunately, no comparison with experiment or with comparable calculations is yet possible.

It is interesting to note that no calculation has been reported for a (111) surface, even though this orientation predominates in polycrystalline Ni samples, which are often used in experiments. The methods used in the calculations cited above are so numerically intensive, that the reduction in computation which results from the extra (in-plane) reflection symmetry of the (100) film has been a major factor in determining the direction of theoretical investigation. Here we compare behavior of (100) and (111) films, surfaces, and interfaces. We find interesting systematic difference between the two orientations.

There is actually a substantial body of theoretical work which is immediately relevant to the problem of magnetic films, and yet whose relevance has not been emphasized. We refer to work on magnetic alloys¹⁷ and impurities.¹⁸ We argue that the suppression of film magnetism by the nonmagnetic substrate is quite analogous to the suppression of impurity magnetism by the nonmagnetic matrix, or of Ni magnetism in alloys by the nonmagnetic constituent. This point is discussed later in the paper.

C. Scope and results of this work

In this paper we present results of calculations for the magnetic and electronic properties of the

ideal Ni (100) and (111) surfaces, the Ni-Cu (100) and (111) interfaces, and ideal epitaxial Ni films of from one to five atomic layers on Cu (100) and (111). The Ni(100) surface has been extensively studied,⁷⁻⁹ and one calculation¹⁰ for a monolayer Ni film on Cu(100) has been reported. Otherwise these results are all completely new. In addition we have performed some numerical "experiments" which illuminate the crucial factors determining film magnetic behavior. From these results, we attempt to extract a coherent picture of the magnetic properties of these systems, which sheds light on the disparate experimental results¹⁻⁵ and suggests possible directions for future experiments.

For our calculations we have employed the simplest techniques consistent with the treatment of real systems. We use a tight-binding scheme, with the exchange interaction treated self-consistently in a single-site approximation. Only properties at temperature $T=0$ are considered. We find excellent agreement with available results of fully self-consistent calculations.

We conclude this introduction by summarizing the most important of our results. The monolayer Ni film on Cu(100) is found to be substantially magnetic, whereas on a Cu(111) substrate it is magnetically dead, or nearly so. The surprising sensitivity to substrate orientation is easily understood in view of other results presented. The Ni magnetization at a Ni-Cu interface is suppressed substantially, by approximately 30%, relative to Ni bulk. On the other hand, the magnetization of an isolated monolayer Ni film is considerably enhanced relative to the bulk. The two effects compete, and they almost cancel each other for the monolayer Ni film on Cu(100). For the monolayer of Ni on Cu(111) the delicate balance of effects is no longer present. For other substrates such as Al, which are expected to couple more strongly to the Ni, a paramagnetic Ni monolayer is expected.

Because of the short screening length, the effect of both the interface and the surface are confined to one or two atomic layers in Ni. Thus for films of four and even three atomic layers, the behavior of the film surface and the film-substrate interface are quite similar to the ideal surface and interface.

We find that the major physical cause of magnetization suppression in the interface and film is hybridization between the Ni d band and substrate conduction band, which affects the projected local DOS at the interface. The same mechanism is responsible for the suppression of Ni magnetization in Ni alloys.¹⁷ Unfortunately, the useful analogy be-

tween alloy and interface has been largely overlooked.

The cause of the *enhancement* in magnetization for isolated thin films is *d* band narrowing and *sp-d* dehybridization, which result from reduced coordination number.

To verify these conclusions, and to learn more about the effect of *sp-d* hybridization, we have artificially varied the coupling between Ni *d* band and substrate conduction band. Such an approach, which bridges the gap between realistic and model calculations, proved highly instructive. The magnetization of a monolayer Ni film is extremely sensitive to the degree of film-substrate coupling, with the realistic Ni-on-Cu case falling in the intermediate regime of coupling strength. If we consider Ni on some substrate, to which it couples more strongly than to Cu, a quite different picture emerges. For one or two layers of Ni, the film is paramagnetic, but for three or more layers the film is ferromagnetic, with an abrupt magnetic transition as thickness is increased. The critical film thickness (for strong film-substrate coupling) is determined by the screening length in Ni, and represents a substrate-independent upper bound for the critical film thickness at which ferromagnetism first appears. This conclusion is supported by experiments^{4,5} which find that for simple metal substrates magnetism appears at a film thickness of 2.5–3 atomic layers.

II. CALCULATION

This section describes our calculations. We used a tight-binding Hamiltonian, with the exchange interaction in the single-site approximation. This is the simplest method consistent with the treatment of real systems. Comparison with available fully self-consistent calculations suggests that our methods are quantitatively reliable. Such comparisons are drawn where appropriate throughout the discussion of results in Sec. III. More important, this work complements the few fully self-consistent results available, by allowing the inclusion of a broader range of systems.

A. The Hamiltonian

We take our Hamiltonian to be the sum of a one-electron term H_0 and an electron-electron interaction term H_{ee} . For H_0 we choose the parametrized tight-binding scheme of Slater and Koster.¹⁹ The Hamiltonian H_0 is written in terms of one- and two-center integrals, which are treated as param-

eters chosen to fit the bulk band structure. We include *s*, *p*, and *d* orbitals, with interactions up to second-nearest neighbor. For the matrix elements between Ni and Cu, we take the geometric mean of the respective Ni-Ni and Cu-Cu matrix elements. The two sets of intersite matrix elements are very similar, so the results are insensitive to the precise scheme for choosing the Ni-Cu matrix elements.

The electronegativities of Ni and Cu are the same to within about 0.1 eV,²⁰ so we choose the zeroes of energy for the two metals so as to line up their bulk Fermi levels. However, the final self-consistent results are not sensitive to physically reasonable (~ 0.2 eV) differences in the respective Fermi levels.

For the electron-electron interaction we use a single-site approximation which has been extensively discussed,²¹

$$H_{ee} = \sum_{i,\sigma,\sigma'} \sum_{\alpha,\beta,\gamma,\delta} U_{\alpha\beta\gamma\delta} c_{i\alpha\sigma}^\dagger c_{i\beta\sigma'}^\dagger c_{i\gamma\sigma} c_{i\delta\sigma}, \quad (1)$$

where $c_{i\alpha\sigma}^\dagger$ creates an orbital of symmetry α and spin σ at site i .

We treat H_{ee} in the Hartree-Fock approach; we can, with some approximations, reduce H_{ee} to a simple form for the on-site potential shifts,

$$\begin{aligned} \Delta E_{d\nu\sigma} = & -\frac{1}{2}(U-J)\langle m_{d\nu\sigma} \rangle - \frac{1}{2}J\langle m_{d\sigma} \rangle \\ & + V_{sd}\langle n_s - n_s^0 \rangle + V_{dd}\langle n_d - n_d^0 \rangle, \end{aligned} \quad (2)$$

$$\Delta E_{s\sigma} = V_{ss}\langle n_s - n_s^0 \rangle + V_{sd}\langle n_d - n_d^0 \rangle.$$

Here $\Delta E_{d\nu\sigma}$ is the on-site potential shift for a *d* orbital of symmetry ν and spin σ , measured relative to the value for the pure paramagnetic metal. By $m_{d\nu\sigma}$ we denote the spin polarization ($n_{d\nu\sigma} - n_{d\nu\bar{\sigma}}$) in the *d* orbital of symmetry ν at a given site, and $m_{d\sigma} \equiv \sum_{\nu} m_{d\nu\sigma}$. The total *d* occupancy at the site is denoted by $n_d \equiv \sum_{\nu,\sigma} n_{d\nu\sigma}$, and the value for the respective pure metal is n_d^0 . Quantities for *s* and *p* orbitals are similarly defined. In (2), *s* refers to the entire *sp* complex.

We define U as the on-site direct Coulomb integral between *d* orbitals of the same symmetry (rescaled by correlation effects, see below), U' is the integral between *d* orbitals of different symmetry, and J is the exchange integral. We define $V_{dd} \equiv U' - \frac{1}{2}J$, which gives the effective (repulsive) interaction between *d* electrons, aside from magnetic effects. We similarly define an effective interaction V_{ss} among *sp* electrons, and V_{sd} between *sp* and *d* electrons. We neglect the on-site exchange in-

tegrals other than between d orbitals. The ratios $U:U':J$ are taken to be 5:3:1 as suggested by Herring²¹; this incidentally allows us to cancel a term involving $U+J-2U'$. These ratios are not crucial. Similar results are obtained for $J=0$ or $J=U$ as long as the absolute magnitude is scaled to give the correct²² bulk Ni magnetization, $\mu=0.616\mu_B$. Such scaling is necessary in any case when we work in the Hartree-Fock approximation, since the effective interaction is reduced by correlation effects.²¹

It is difficult within the tight-binding approximation to treat charge transfer accurately at the surface. To avoid this problem and still treat charge transfer and potential shifts at the surface in a simple way, we impose upon our potential the constraint

$$\Delta n_{sp} = \Delta n_d = 0. \quad (3)$$

That is, the average on-site potential of the d orbitals, and of the s and p orbitals, are fixed by the requirement that the total occupancies of the sp and d complexes at any site not differ from the bulk values. More fully self-consistent calculations^{11,23} suggest a transfer of about 0.1 electrons per atom from the sp band to the d band at the surface. By neglecting this, we may expect to exaggerate the surface magnetization by roughly $0.1\mu_B$ per atom, an acceptable level of error.

B. Evaluation of electronic properties

In calculating electronic properties of surfaces, it is usual to replace the real semi-infinite geometry with a thin "slab" of a few atomic layers. For example, the most sophisticated calculations^{8,9} for the Ni surface reported to date have been limited to (100) films of five atomic layers. Wang and Freeman,⁷ using a somewhat less fully self-consistent method, have treated a nine-layer film. Many electronic properties are not sensitive to film thickness; the magnetic behavior of a (100) film proves to be an exception.

In these calculations we have used two complementary methods. One is the usual slab method; the other is a Green's-function method, developed elsewhere,²⁴ which permits us to treat a semi-infinite geometry. We find that a realistic semi-infinite geometry has a significant effect on the results for magnetization *only* for the case of the ideal Ni(100) surface.

Spin oscillations are relatively long ranged because they are not screened. For a Ni film on a Cu substrate, the Ni-Cu interface imposes a correct

boundary condition on the oscillations; since there is effectively no penetration of the magnetization into the Cu, the thickness of the Cu substrate is relatively unimportant.

Because the Green's-function method is less widely used than the slab method, we sketch out the essential points. Let $\phi_{i\mathbf{R}}$ denote the i th local orbital, centered on lattice site \mathbf{R} . Also let $\vec{\mathbf{R}}_m$ denote a lattice vector lying in the m th plane of atoms from the surface. For our basis we take Bloch sums in a single plane,

$$\phi_{im}(\vec{\mathbf{k}}) = N^{-1/2} \sum_{\mathbf{R}} \phi_{i\mathbf{R}m} \exp(i\vec{\mathbf{k}} \cdot \vec{\mathbf{R}}_m),$$

where $\vec{\mathbf{k}}$ is a wave vector parallel to the surface, and N is the number of atoms in a layer.

The Green's function is defined by Dyson's equation, which for our one-electron Hamiltonian is simply $I = (\epsilon - H)G$. We handle the orbital indices implicitly in matrix notation, but write the layer indices explicitly as subscripts. For example, $\tilde{G}_{mn}(\vec{\mathbf{k}}, \epsilon)$ is a matrix such that

$$[\tilde{G}_{mn}(\vec{\mathbf{k}}, \epsilon)]_{ij} \equiv \langle \phi_{im}(\vec{\mathbf{k}}) | G(\epsilon) | \phi_{jn}(\vec{\mathbf{k}}) \rangle.$$

Then Dyson's equation leads to an infinite set of simultaneous equations involving different layers.

For example, with only neighboring layers interacting, we can write

$$\begin{aligned} \tilde{I} &= (\epsilon - \tilde{H}_{11})\tilde{G}_{11} - \tilde{H}_{12}\tilde{G}_{21}, \\ 0 &= (\epsilon - \tilde{H}_{22})\tilde{G}_{21} - \tilde{H}_{21}\tilde{G}_{11} - \tilde{H}_{23}\tilde{G}_{31}, \\ 0 &= (\epsilon - \tilde{H}_{33})\tilde{G}_{31} - \tilde{H}_{32}\tilde{G}_{21} - \tilde{H}_{34}\tilde{G}_{41}, \end{aligned} \quad (4)$$

and so on. To uncouple these equations we note that in the bulk, the relation between Green's-function matrix elements for successive layers must be independent of the particular layer. We therefore define the transfer matrix $\tilde{T} = \tilde{G}_{m+1,n}(\tilde{G}_{m,n})^{-1}$, which is independent of m and n , for m sufficiently large. The transfer matrices for each $\vec{\mathbf{k}}$ and ϵ may be calculated once and stored.

In Eqs. (4) above, we include self-consistency only as a shift in the diagonal elements of the Hamiltonian. For example, if we treat two layers self-consistently, i.e., only H_{11} and H_{22} differ from the bulk value, then \tilde{G}_{31} is related to \tilde{G}_{21} by an equation with only bulklike terms, and we can write $\tilde{G}_{31} = \tilde{T}\tilde{G}_{21}$. Thus we uncouple the infinite set (4) of equations, and reduce it to two simultaneous matrix equations.

Once we have \tilde{G}_{mm} for the layers of interest, it is trivial to define the local density of states and local occupancy. For example, we can define a partial density of states $D_{md}(\epsilon)$ in which we project out the contribution from the d orbitals in layer m ,

$$D_{md}(\epsilon) = -\frac{1}{\pi} \text{Im} \sum_k \text{Tr}_d \tilde{G}_{mm}(\vec{k}, \epsilon),$$

where Tr_d denotes a partial trace, taken only over the indices corresponding to d orbitals. The d occupancy on a site in layer m is

$$n_d = \int_{-\infty}^{\epsilon_F} D_{md}(\epsilon) d\epsilon.$$

C. Accuracy

Here we discuss, first, the numerical accuracy of our calculations, and second, the crucial approximations in our Hamiltonian and their effect on the reliability of the model.

Magnetic surface calculations pose unusual problems for numerical convergence. A significant portion of the magnetization at the surface may derive from surface states which intersect the Fermi level. In this case the magnetization converges rather slowly with respect to wave-vector sample.²⁵ For example, for the (100) surface, 15 wave vectors in the surface Brillouin zone gave excellent convergence for bulk properties (obtained by using a thick slab with periodic boundary conditions); however on increasing the sample to 21 wave vectors, the Ni-Cu (100) interface magnetization changed by 10%, because of better resolution of interface states. We obtained good convergence of all properties using 21 wave vectors in the irreducible wedge of the (100) surface Brillouin zone, and 30 wave vectors in the (111) irreducible wedge.

Convergence of the potential can also be somewhat tricky for inhomogeneous magnetic systems. For a paramagnetic calculation, a small error in the input potential (relative to the self-consistent value) gives rise to a small error in the charge density; this in turn results in a *large* change in the calculated output potential, on account of the large Coulomb restoring forces. Thus good agreement between input and calculated output potential ensures that the input potential and calculated charge density are very close indeed to the self-consistent values. On the other hand, while a small error in *charge* density gives rise to a large restoring force, a small error in *spin* density has the opposite effect. Increasing the spin polarization beyond its equilibrium value results in a stronger exchange splitting, which reduces

the exchange energy. The “restoring force” is the deviation from a weak minimum in the *sum* of “band” energy and exchange energy, and so is not directly reflected in the potential. Thus the magnetization can “drift” over many iterations with little apparent change in the degree of convergence, as judged by the potential. Because the methods used here are relatively inexpensive, we were able to ensure in every case that our results were well converged. In particular, our potentials were converged to 10^{-4} Ry, and the magnetizations were seen to converge exponentially with iteration, so that final values were numerically reliable to roughly $3 \times 10^{-3} \mu_B$ or better.

We now recapitulate the most crucial approximations in our Hamiltonian, and consider their effects. The most drastic approximation here is (3), in which the self-consistent change in the potential is approximated by an on-site term, determined by imposing a zero-charge-transfer condition on the sp - and d -projected subbands separately at each site. Comparison with fully self-consistent calculations^{11,23} suggests that this is an excellent approximation. Still, the uncertainty of up to 0.1 electron in the local d occupancy corresponds to a possible error of up to $0.1 \mu_B$, which is significant for Ni systems. However, there is no evidence that any available methods are accurate to better than $0.1 \mu_B$ for inhomogeneous systems in any case. Approximation (3) also neglects the crystal-field splitting of the on-site potential.

Our Hartree-Fock treatment necessarily exaggerates the exchange splitting, which is reduced by correlation effects. This is not a serious problem for bulk calculations, where the majority-spin band is essentially full. For heterogeneous systems, where the majority-spin band may be less full at some sites, the exaggerated exchange splitting could conceivably be a source of error in the magnetization.

Finally, the use of a tight-binding Hamiltonian should be analyzed with care. This method provides a rather good treatment of the d band, but the handling of the sp band is less accurate. Since sp - d hybridization plays an important role here, the tight-binding approximation introduces some risk of reduced quantitative accuracy.

We must ultimately base our assessment of overall accuracy upon comparison with reported results of fully self-consistent calculations for simple systems, and with experiment. Such comparisons are few, but they suggest that our methods are reliable even for the quantitative magnetization of

heterogeneous systems. Moreover, the most important results here are trends and comparisons of different systems; *differences* between comparable systems (e.g., different surface orientations) should be much more reliable than absolute magnetization. It is our hope that this work will stimulate experiments to test our conclusions.

III. RESULTS

The discussion of results is divided into four parts. Section IIIA treats the ideal Ni (100) and (111) surfaces. Besides presenting results for the magnetization and electronic structure, we introduce the basic ideas used later.

Section IIIB presents results for the Ni-Cu interface. In addition to its intrinsic interest, an understanding of ideal interface magnetic behavior is helpful in analyzing results for thin films, where several effects are present at once.

Section IIIC discusses results for thin Ni films on Cu. By considering a range of thicknesses, we follow the evolution of magnetic behavior from the Ni monolayer to the thick-film limit, where the surface and interface decouple.

Finally, in Sec. IIID we present results of some numerical "experiments." By artificially altering the film-substrate coupling, we are able both to isolate the essential physical mechanism acting to suppress film magnetization, and to understand the qualitative effect of varying substrate composition.

A. The ideal Ni surface

Previous theoretical investigations of the surface magnetism of Ni (Refs. 7–9) focused exclusively on the (100) surface, even though the (111) surface is energetically favored. In our discussions we stress the systematic differences between these two surfaces. The ideas developed also prove fruitful in understanding the magnetic behavior of ultrathin Ni films.

Table I summarizes our results for the layer-by-

TABLE I. Spin polarization by layer at Ni surface ($n_{\uparrow} - n_{\downarrow}$ per atom).

Layer	(100)	(111)
<i>S</i>	0.74	0.65
<i>S</i> –1	0.55	0.62
<i>S</i> –2	0.56	0.56
Bulk	0.56	0.56

layer magnetization at ideal Ni (100) and (111) surfaces. The spin polarization at the surface is probably exaggerated by our approximation (3), as discussed above.

The most interesting feature of these results is the difference in magnetization between the two surfaces. The spin polarization of the (100) surface is significantly stronger. While we know of no unambiguous experimental determination of the relative magnetization of the two surfaces, the results of Rau² suggest a possible confirmation of our result.

Figure 1 shows the majority- and minority-spin density of states (DOS) of bulk Ni for comparison with layer-projected results presented below. As in all the DOS plots in this paper, we have projected out *only* the contribution from the *d* orbitals, and we have smoothed the DOS by convolution with a Gaussian of halfwidth of 0.08 eV at half height.

Figure 2 shows the spin-projected DOS at the Ni (100) and (111) surfaces. There are two differences between the (100) and (111) results which explain the larger (100) surface magnetization. First, the (100) surface DOS is narrower than the (111) DOS. This may be simply a consequence of lower coordination; in the fcc lattice an atom has eight nearest neighbors at the (100) surface versus nine at the (111) and 12 in the bulk. Also, the (100) surface DOS has a very sharp upper *d*-band edge. These factors result in a large DOS at the Fermi level E_F which is conducive to a large magnetization.

The second important difference between the (100) and (111) results lies in the high-energy tail of the DOS. Recall that we have projected out only the *d*-orbital contribution, which extends well above the *d*-band "edge" due to hybridization with *sp*-like (free-electron-like) states. This high-energy "hybridization tail" of the *d* band tends to reduce the magnetization. By preventing the complete filling of the majority-spin *d* band, it inhibits polarization of the available *d* holes. This hybridization tail is

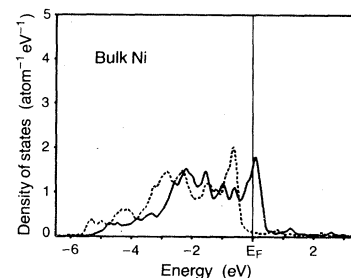


FIG. 1. *d*-orbital component of the density of states of bulk Ni metal. Broken line, majority spin; solid line, minority spin.

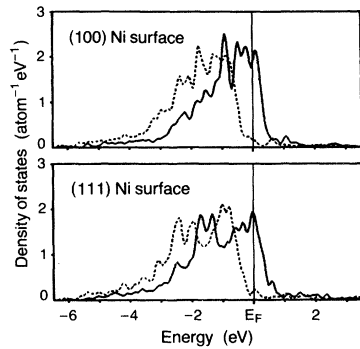


FIG. 2. *d*-orbital components of the density of states, projected at a site at ideal Ni surfaces. Top, (100) surface; bottom, (111). Broken line, majority spin; solid line, minority spin.

suppressed at the (100) surface. There is a dehybridization of the *sp* and *d* bands there, which contributes to the (100) surface magnetization. (The difference appears very small visually, since the scale of the figure is determined by the *d* band, which contains five electrons. We are, however, concerned with shifts of much less than 0.1 electron from one spin band to the other.) This *sp-d* dehybridization probably also contributes to the narrowing of the DOS at the (100) surface.

Figures 3 and 4 show the dispersion of surface states and surface resonances at the (100) and (111) surfaces, respectively. The two-dimensional surface Brillouin zones and the labeling of symmetry points are also shown. Because a small change in the po-

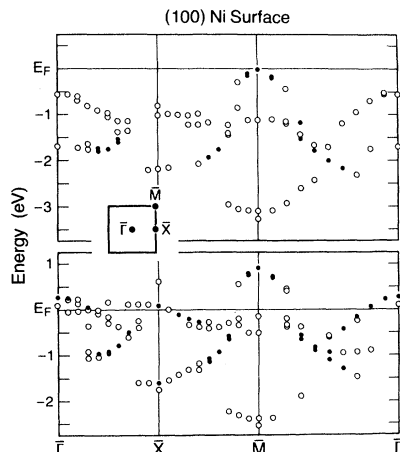


FIG. 3. Surface states and resonances at the surface of a seven-layer Ni(100) slab. Top and bottom are majority and minority spin, respectively. Solid circles denote states which are over 80% localized in the surface layers; open circles denote states with weights at the surface layers between 40% and 80%. Inset: (100) surface Brillouin zone.

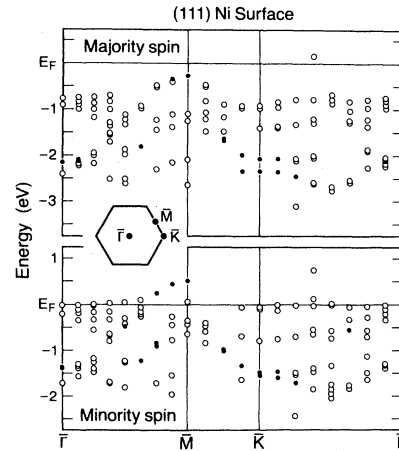


FIG. 4. Surface states and resonances at the surface of a seven-layer Ni(111) slab. Top and bottom are majority and minority spin, respectively. Solid circles denote states which are over 80% localized in the surface layers; open circles denote states with weights at the surface layers between 40% and 80%. Inset: (111) surface Brillouin zone.

tential can change a resonance into a bona fide surface state, or vice versa, we have made no attempt to distinguish the two precisely. Instead, we consider a seven-layer Ni slab. For a given (two-dimensional) wave vector we plot a solid circle for each eigenstate which is over 80% localized in the surface layers of the slab, and an open circle if the state is between 40% and 80% surface localized. We make no attempt to correct or suppress the small spurious doubling which results from mixing of surface states localized on the two surfaces. Such an analysis, while of only limited use for comparison with photoemission results, is the clearest way to draw the connection between surface states and resonances, and the local DOS at the surface.

The (100) results show a wealth of surface states and resonances near the Fermi level. These contribute to the large local DOS at E_F for the surface. The (111) surface does not display surface states near E_F , except in the vicinity of the symmetry point \bar{M} .

Our results for the relative position and dispersion of the surface states and resonances appear to be in excellent agreement with those of Wang and Freeman.⁷ While a detailed comparison is difficult because of the manner in which those results were presented, the evident overall agreement is encouraging. There is, however, a significant difference in the overall position of the two sets of spin bands, for two reasons. First, our Hartree-Fock calculation overestimates the exchange splitting, which

is reduced by correlation effects. These effects are included in an approximate way in the local-density-functional calculation of Wang and Freeman. Second, our results give a somewhat larger surface magnetization than Wang and Freeman, adding to the difference between our exchange splitting and theirs. A larger surface magnetization is consistent however with more recent calculations^{8,9}; approximation (3) doubtless also contributes to the discrepancy.

The Ni(100) surface results in Fig. 3 give the appearance of rather well-defined two-dimensional surface bands. One can follow the dispersion of a given resonance across the whole Brillouin zone in several cases. The (111) surface results of Fig. 4 display less structure, with many "bulk" states contributing more or less equally to the surface-projected band structure.

Many of the results noted so far suggest that the (100) surface exhibits more quasi-two-dimensional behavior than the (111). This is evidenced in the surface bands, strong magnetization, and *sp-d* dehybridization, which are reminiscent of unsupported monolayer behavior.^{10,11}

Finally, we call attention to an interesting symmetry-related feature of the surface bands. Both the (100) and (111) surfaces exhibit surface states which split off the top of the *d* band at the symmetry points \bar{M} . (The coincidence of labeling, determined by established convention, is accidental.) For the (100) surface, \bar{M} corresponds to the projection of the line *W-X* in the fcc bulk Brillouin zone. There is an extremely flat bulk band along this line. For the relevant *d*-state symmetry, the nearest-neighbor interaction between layers vanishes. Therefore, at \bar{M} , a small change in potential at the surface is sufficient to create a surface state. As one moves away from \bar{M} , the layer decoupling disappears. The peculiar dispersion of the surface state at \bar{M} is attributable to the wave-vector-dependent coupling between layers, and cannot be understood in a strictly two-dimensional model.

In the (111) surface the surface state at \bar{M} has a similar origin. In that case, \bar{M} corresponds to the

line *L-X* in the bulk, where there is again an extremely flat band. (Unlike *W-X*, this symmetry-related flat band has not been previously discussed, since it does not fall on the symmetry lines traditionally used in plotting fcc band structures.)

B. The Ni-Cu interface

While much experimental¹⁻⁵ and theoretical¹⁰ attention has been paid to the magnetic behavior of thin films, such work has often emphasized the supposed analogy between film and surface, while neglecting the film-substrate interface. We argue that the surface and the film-substrate interface have radically different and competing effects on film magnetism. Thus it is of great importance to understand the magnetic behavior of the interface between a ferromagnet and a normal metal, before attacking the conceptually more complex film problem.

We approach the interface problem by considering thin Cu films on a Ni (100) or (111) substrate. These systems are of particular interest because ideal (surface insensitive) interface behavior develops after only one or two atomic layers of Cu have been deposited. The interface is therefore accessible to such sensitive probes as photoemission and spin-polarized electron diffraction. Moreover, Cu is easily deposited on Ni in almost perfect epitaxial layers. (For Ni on Cu it is difficult to avoid clumping of the Ni atoms and diffusion of the Ni into the Cu bulk.)

The method of calculation has been discussed in detail above. Results for the layer-by-layer Ni spin polarization at the (100) and (111) Ni-Cu interface are given in Table II, for Cu films of one and two atomic layers on Ni. The magnetization in the Cu is in every case negligible ($\leq 0.02\mu_B$, almost entirely caused by the small negative polarization of the *sp* band).

The results in Table II show that the magnetization at the interface is reduced substantially, about 30%, from the bulk value. The effect does not

TABLE II. Spin polarization of Ni layers at Ni-Cu interface ($n_{\uparrow} - n_{\downarrow}$ per atom).

Ni layer	(100)		(111)	
	Cu(1)-Ni	Cu(2)-Ni	Cu(1)-Ni	Cu(2)-Ni
<i>I</i>	0.39	0.37	0.43	0.38
<i>I</i> - 1	0.51	0.50	0.54	0.54
<i>I</i> - 2	0.57	0.57	0.57	0.57
Bulk	0.56	0.56	0.56	0.56

differ much between the (100) and (111) interfaces, though the sensitivity to Cu thickness is slightly greater for the (111) interface. Even for the (111) interface, a single atomic layer of Cu on Ni provides a reasonable approximation to the ideal interface for experimental purposes.

The effect of the interface on magnetization is large only in the first Ni layer, and is negligible ($\leq 0.02\mu_B$) at the third and more distant layers. Note that because of approximation (3), the results presented here tend to underestimate the suppression of the magnetization at the interface. In a previous calculation without this approximation,²⁶ we found that local band narrowing at the interface caused a transfer of almost 0.1 electrons from the *sp* orbitals into the *d* orbitals in the Ni interface layer. This local *d*-band filling contributed to the larger suppression of interface magnetization ($\sim 50\%$) reported there, though subsequent improvements in our wave-vector sample also contribute to the difference.

The cause of the reduced local magnetization at the interface can be seen in Fig. 5, which shows the local *d*-projected DOS in the Ni interface layer for the (100) and (111) interfaces. The most apparent change from the bulk DOS (Fig. 1) is that the interface DOS has become rounded, losing the sharp upper *d*-band edge seen in the bulk. Elsewhere, in treating the Ni-Cu alloy,¹⁷ we have discussed the importance of this sharp band edge for the ferromagnetism of Ni. For a band with a "tail" in the DOS, it is difficult to achieve saturation, i.e., one spin band completely full; whereas, in a Stoner-type rigid-band model, if the DOS of a ferromagnet is constant with a sharp cutoff, the spin polarization will always proceed to saturation.

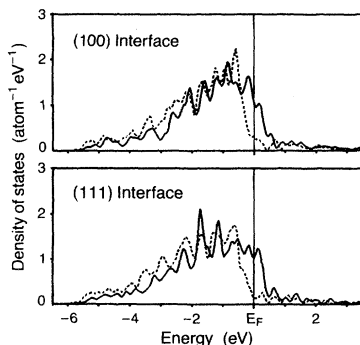


FIG. 5. *d*-orbital component of the density of states, projected at a site in Ni interface layers of Ni-Cu interfaces. Top, (100) interface; bottom, (111). Broken line, majority spin; solid line, minority spin.

We must emphasize that the interface behavior is entirely analogous to that of the Ni-Cu alloy.¹⁷ Both systems share the characteristic changes in projected Ni *d*-band shape caused by reduced local symmetry, reduced Ni-Ni coordination number, and enhanced *sp-d* hybridization.

The validity of the analogy between alloy and interface appears to be experimentally confirmed by recent studies²⁷ of compositionally modulated Ni-Cu epitaxial-film structures. In these systems, alternating films of Ni and Cu are deposited in turn. The structure is then annealed to allow interdiffusion of the Cu and Ni. The smooth crossover observed, between the sharp-interface regime and the compositionally-modulated-alloy regime, suggests that there is no fundamental difference between the important mechanisms in these two cases.

It is important to notice that, from the point of view of the *d* orbitals alone, the Ni surface and Ni-Cu interface are very similar. The Cu *d* band is centered well below the Fermi level, and because of the large energy denominator the Cu *d* orbitals have almost negligible interaction with the states near E_F . We have verified this explicitly by artificially removing the Cu *d* orbitals from the Hamiltonian, and finding insignificant change ($\sim 0.02\mu_B$) in the interface magnetization. Thus, considering the *d* orbitals alone, a Ni atom interacts only with its Ni neighbors at the Ni-Cu interface, just as at an ideal Ni surface.

It is the interaction between the Ni *d* orbitals and the free-electron-like *sp* states which accounts for the radical difference in magnetic behavior between the two geometries. This interaction tends to broaden and "smear" the *d* band. Comparison of the surface *d*-band DOS (Fig. 2) with the interface DOS (Fig. 5) shows that at the interface the *d* band is broadened and rounded, relative to the surface. In particular, the upper edge of the minority-spin band is less sharp at the interface, resulting in a reduced DOS at E_F . These changes are caused entirely by the greater *sp-d* hybridization at the interface.

We have also looked for interface states at the (100) and (111) Ni-Cu interfaces. The interface states and resonances are shown in Figs. 6 and 7. We find no evidence of interface states or interesting resonance, *except* for states near \bar{M} in the Brillouin zone for both surfaces. These states are similar to those at the surface, discussed at the end of Sec. III A. Because of the symmetry-induced decoupling of successive layers, even the interface resonances are similar to those at the surface, discussed at the end of Sec. III A. Because of the symmetry-induced decoupling of successive layers, even the interface resonances are similar to those at the surface, discussed at the end of Sec. III A. Because of the symmetry-induced decoupling of successive layers, even the interface resonances are similar to those at the surface, discussed at the end of Sec. III A.

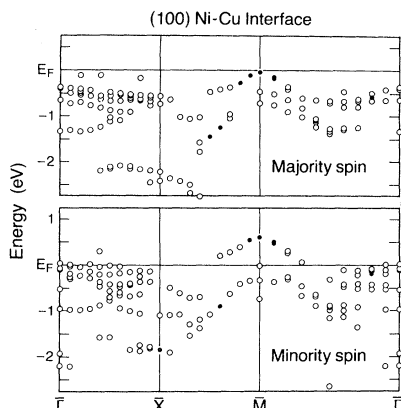


FIG. 6. Interface states and resonances at the Ni interface layer of a six-layer Ni(100) slab with one layer Cu on each face. Solid circles denote states which are over 80% localized in the Ni interface layers; open circles denote states with weights at the Ni interface layers between 40% and 80%.

C. Thin Ni films on Cu (100) and (111)

While several fascinating experiments probing Ni film magnetism have been reported,¹⁻⁵ the theoretical understanding of ultrathin films is in its infancy. Only one self-consistent calculation for a real system has been reported—Wang *et al.*¹⁰ have studied a monolayer Ni film on Cu(100). Here we present the first investigation of the roles of film thickness and substrate orientation (crystal face) in determining the magnetic and electronic properties of the films. Section III D below examines the role of substrate composition in a qualitative way.

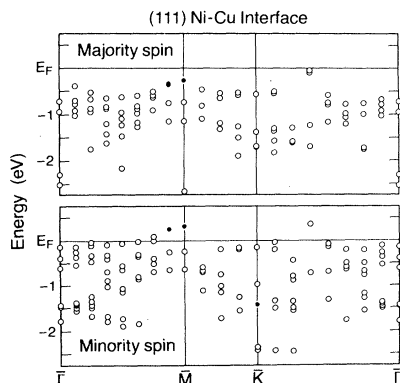


FIG. 7. Interface states and resonances at the Ni interface layer of six-layer Ni(111) slab with one layer Cu on each face. Solid circles denote states which are over 80% localized in the Ni interface layers; open circles denote states with weights at the Ni interface layers between 40% and 80%.

Results for the layer-by-layer spin polarization of Ni films of from one to five atomic layers, on Cu (100) and (111) substrates, are presented graphically in Fig. 8, which also includes data from Tables I and II for the surface and interface magnetization; these correspond to the limit of infinite film thickness.

Each data point in Fig. 8 gives the spin polarization of one layer in the respective film. In these results the magnetization decreases monotonically from surface to interface; the only exceptions are unimportant, and correspond to Friedel oscillations in layers in the interior of thicker films, which have nearly equal polarization. We therefore omit labeling of the individual points.

The first result to notice concerns the presence or absence of magnetically “dead” layers. For the (100) surface, we find no evidence of such dead layers; even the monolayer film has its moment reduced only about $0.1\mu_B$ relative to Ni bulk. This is in excellent agreement with the only fully self-consistent calculation reported for a supported Ni film; there, Wang *et al.*¹⁰ found a reduction in the magnetization of a monolayer Ni film on Cu(100) of slightly over $0.2\mu_B$. The discrepancy of $0.1\mu_B$ is consistent with the level of accuracy expected from approximations such as (3), and is typical of the agreement among various *a priori* calculations.⁷⁻⁹

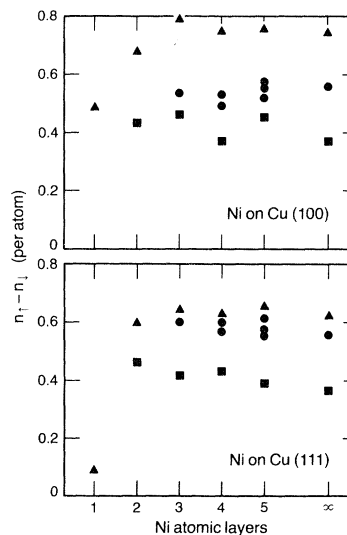


FIG. 8. Layer-by-layer spin polarization of epitaxial Ni films of thicknesses from one to five atomic layers, on Cu(100) (top) and Cu(111) (bottom). Triangle, surface layer; square, interface layer; circle, interior layers of film. The three data points for the limit of infinite film thickness correspond to ideal surface, bulk, and interface.

For the (111) films, the situation is radically different. While the magnetic behavior varies smoothly with film thickness down to two atomic layers, at a single layer the magnetization drops abruptly to less than $0.1\mu_B$. In view of the fact that our approximations consistently overestimate surface magnetization, this result is consistent with a magnetically dead Ni monolayer on Cu(111). Finite temperature would probably kill such weak ferromagnetism in any case.

The surprising sensitivity of the film magnetization to substrate orientation is attributable to the delicate balance here between competing effects. Calculations^{10,11} for an isolated Ni film find a magnetization substantially greater than in bulk Ni. On the other hand, coupling to the substrate tends to suppress the magnetization. For the Ni monolayer on Cu(100) there is a substantial cancellation between these competing effects. Any change in the film electronic structure can upset this fortuitous balance, and drastically change the magnetization.

For thicker films, the magnetization of the interior layers tend to cluster closely around the bulk value, with substantial changes in magnetization restricted to the surface and interface layers. Only for films of one or two layers, where there are no "interior" layers, does this simple picture break down.

It is interesting to note that the interface magnetization displayed in Fig. 6 exhibits substantial oscillations with film thickness for the (100) films, but very little for the (111) films. This illustrates the sensitivity of Ni(100) films to thickness-imposed boundary conditions. In calculations where (100) slabs are used^{7-9,16} to mimic the ideal surface, this sensitivity poses a problem. We have performed such slab calculations, and find that the Friedel-type spin oscillations are not noticeable for (111) slabs. Thus a five-layer slab provides a good approximation for the (111) surface, while for the (100) surface even a seven-layer slab noticeably exaggerates the spin oscillations. Only for the thinnest films does the film behavior deviate qualitatively from that of the ideal surface and interface; we therefore discuss in detail the electronic structure only of the monolayer films.

Figure 9 shows the d -projected local DOS in the Ni monolayer films, decomposed by spin. The (100) monolayer has a very narrow d band with a sharp upper band edge and a large DOS at E_F . The (111) monolayer DOS is broad by comparison ("fragmented" might be a better word), and exhibits a small peak above the main band, resulting in a rather

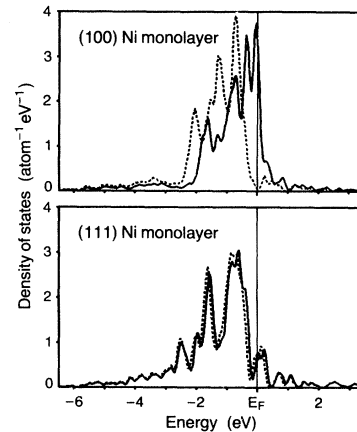


FIG. 9. d -orbital component of the density of states, projected at a Ni site in a Ni monolayer film on Cu. Top, (100) monolayer; bottom, (111). Broken line, majority spin; solid line, minority spin.

small DOS at E_F . Moreover, the (111) monolayer appears to show a stronger hybridization tail in the d -projected DOS than the (100), which also may play an important role in determining the weakness or nonexistence of Ni(111) monolayer magnetism.

The dispersion of surface states and resonances in the monolayer films are shown in Figs. 10 and 11. For the (100) monolayer film, a very flat band of surface states along $\bar{\Gamma}$ - \bar{X} gives rise to the sharp upper band edge in the DOS. In contrast, the only film-localized states at E_F for the (111) monolayer belong to the steeply dispersing surface state around \bar{M} , and so the local DOS at E_F is small.

The symmetry-related surface states at the points \bar{M} in the (100) and (111) surface Brillouin zones were discussed above in the context of the ideal surface and interface; in the monolayer film these states split off from the continuum in a dramatic way. Unfortunately at \bar{M} , where the states are most localized, they lie above E_F and are not observable in photoemission experiments.

D. Model film systems

In the preceding section we emphasized the role of the nonmagnetic substrate in suppressing Ni film magnetization. We have, moreover, asserted that sp - d hybridization is the most important mechanism determining film magnetization. The degree of hybridization depends on the strength of the coupling between Ni d and substrate sp bands; we anticipate that this coupling is stronger for normal met-

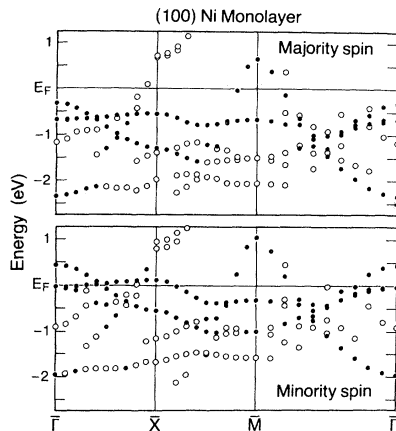


FIG. 10. Surface states and resonances at the monolayer Ni film, for a four-layer Cu(100) slab with one layer of Ni on one side. Solid circles denote states which are over 80% localized in the Ni monolayers; open circles denote states with weight at the Ni monolayers between 40% and 80%.

als than for noble metals, and this explains the greater effectiveness of Al substrates, compared to Cu, in suppressing film magnetism.

In this section we report results of numerical “experiments.” In the first experiment, we artificially vary the strength of the coupling between the Ni-film d band and substrate conduction band; in the second, we examine the thickness dependence of film magnetization in the case of relatively strong film-substrate coupling. The results nicely illustrate both the crucial role of $sp-d$ hybridization, and the qualitative effects of varying substrate composition.

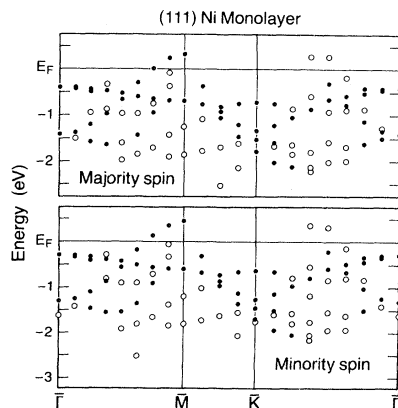


FIG. 11. Surface states and resonances at the monolayer Ni film, for a four-layer Cu(111) slab with one layer of Ni on one side. Solid circles denote states which are over 80% localized in the Ni monolayers; open circles denote states with weight at the Ni monolayers between 40% and 80%.

To vary the film-substrate coupling, we multiply each matrix element in the Hamiltonian which couples Ni d orbitals to substrate s and p orbitals, by a factor t . Thus $t=1$ corresponds to the realistic Ni-on-Cu case, whereas $t>1$ gives an artificially enhanced coupling. For the Ni monolayer on Cu(100), we performed self-consistent calculations of Ni magnetization for various values of t . The results are given in Fig. 12. (For these calculations we sampled 15 wave vectors in the irreducible surface Brillouin zone.)

The realistic Ni-Cu case, $t=1$, has already been discussed. As the film-substrate coupling t is increased, the magnetization drops rapidly until, for $t \geq 1.8$, the film magnetization has completely disappeared. Thus the absence of magnetically dead layers of Ni on Cu is consistent with the existence of such layers on other substrates.

As t is reduced below one, the magnetization increases to well above the Ni bulk value. This illustrates that, in the *absence* of coupling to a substrate, a monolayer Ni film should exhibit *enhanced* magnetization, in accord with calculations^{10,11} for hypothetical isolated Ni film. The magnetization of a real, supported Ni film is determined by the competition between thickness-induced enhancement and substrate-induced suppression of the magnetization.

We point out that the similarity of the spin polarization of a Ni monolayer on Cu(100) to the bulk spin polarization must be viewed as fortuitous. Two large effects almost cancel; but as illustrated in Fig. 12, a change in the effective coupling strength can upset the balance. This is why merely switching from a (100) to a (111) substrate orientation can so drastically change the net result.

Several elegant experiments^{4,5} have examined the onset of ferromagnetism with Ni film thickness on simple-metal substrates. In order to examine the qualitative differences between this case and the

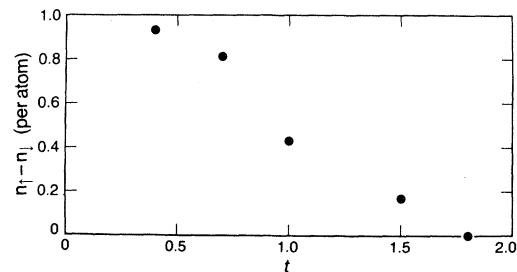


FIG. 12. Spin polarization of a Ni monolayer on Cu(100), as a function of the (artificially altered) coupling t between the Ni d band and the substrate conduction band.

case of a noble-metal substrate, we have calculated the magnetization of Ni(111) films of thickness from one to five layers, for the case of strong ($t=3$) film-substrate coupling. Results are presented in Fig. 13.

The most striking feature here is the sudden onset of magnetization with film thickness. The one- and two-layer films are paramagnetic, yet the three-layer film is similar to the thicker films in its magnetization. This behavior is consistent with the abrupt onset of magnetization observed experimentally.^{4,5}

Note that for the thicker films, the suppression of magnetization is confined to the interface region. Such behavior is to be expected, in view of the short screening length in metals. We might therefore expect that the critical film thickness for the onset of magnetization is determined (in the case of large film-substrate coupling) by the screening length rather than by the coupling strength. To test this hypothesis, we repeated the calculation for the three-layer film, using a very large film-substrate coupling, $t=9$. This large increase in coupling strength resulted in a small (20%) reduction in the magnetization of the middle Ni layer, relative to the $t=3$ case. The surface layer changed only 3%, and the interface layer is effectively paramagnetic in both cases. This suggests that the observed^{4,5} appearance of ferromagnetism at three atomic layers of Ni or less represents a universal, substrate-independent phenomenon (once the nickel-substrate coupling reaches its strong-coupling limit).

In conclusion, these numerical experiments reveal several important points. First, the coupling of film and substrate via $sp-d$ hybridization is the crucial physical effect suppressing film magnetization. Second, the film magnetization, for the case of

monolayer films, is extremely sensitive to the strength of the film-substrate coupling, and hence is strongly dependent on substrate composition. Third, for thicker films the substrate effect is limited to roughly two layers, independent of coupling strength (i.e., independent of substrate composition). Films of three atomic layers or more should therefore be magnetic, regardless of the substrate.

IV. CONCLUSION

By means of simple calculations for a variety of systems, we have developed a clear, consistent picture of the magnetic behavior of Ni films, surfaces, and interfaces. The main qualitative features of the results can be understood in terms of two competing effects: *suppression* of Ni magnetization due to increased $sp-d$ hybridization when a Ni atom is adjacent to noble or normal-metal atoms, and *enhancement* of Ni magnetization due to d -band narrowing and $sp-d$ dehybridization at sites of low coordination number.

Our results are consistent with all the experiments we know of (except perhaps that of Liebermann *et al.*,¹ as discussed in Sec. IA), and serve to identify the factors responsible for the dramatic differences among different experiments. In particular, we have shown that the dependence of film magnetization on substrate composition can explain the various experimental results.

Our analysis suggests two experiments which would be helpful in tying together previous results. First, the magnetization of Ni on Cu could be studied down to monolayer and submonolayer coverage on well-characterized Cu(100) and, especially, Cu(111) surfaces. Second, a systematic investigation of the role of substrate composition in determining film magnetization is greatly needed. Our results suggest that trends in film magnetization with substrate composition will follow trends in Ni alloy magnetization with composition of the non-magnetic components of the alloy.

Finally, we should add a word about the relevance of these results to other magnetic materials. The major factor acting to suppress Ni magnetization at the Ni-Cu interface is $sp-d$ hybridization, which changes the shape of the band edge and reduces the "effective" number of d holes. These effects are important because the Ni d band is almost full, with the Fermi level close to the upper band edge. For metals such as Fe and Mn, with more holes in the d band, the precise shape of the

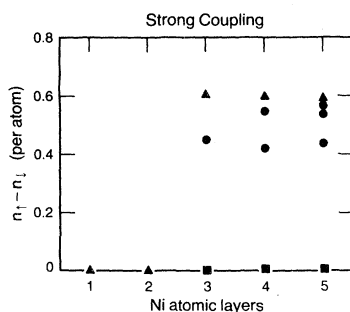


FIG. 13. Layer-by-layer spin polarization for Ni films of thickness from one to five atomic layers, on a (111) substrate. The film-substrate coupling is enhanced by a factor of $t=3$ from the realistic Ni-Cu value. Symbols are as for Fig. 8.

band edge is unimportant; and *sp-d* hybridization has a relatively small effect on the middle of the band. This explains why metallic substrates are not effective in suppressing the magnetization of even submonolayer Fe films.^{4,5}

Note added in proof. Wang *et al.* have recently extended the calculation of Ref. 10 to include two layers Ni on Cu(100) [Phys. Rev. B **26**, 1340 (1982)]. Their results are in very good agreement with ours. O. Jepsen, J. Madsen, and O. K. Andersen have recently reported very detailed results for

unsupported one-, three-, and five-layer Ni(100) "slabs" [Phys. Rev. B **26**, 2790 (1982)].

ACKNOWLEDGMENTS

This work was supported by the Director, Office of Energy Research, Office of Basic Energy Sciences, Materials Sciences Division of the U. S. Department of Energy under Contract No. DE-AC03-76SF00098. The financial support of the Exxon Education Foundation is gratefully acknowledged.

*Present address: Bell Laboratories, Murray Hill, NJ 07974.

¹L. Liebermann, J. Clinton, D. M. Edwards, and J. Mathon, Phys. Rev. Lett. **25**, 323 (1970).

²C. Rau, Comments Solid State Phys. **9**, 177 (1980).

³D. T. Pierce and H. C. Siegmann, Phys. Rev. B **9**, 4035 (1974).

⁴G. Bergmann, Phys. Rev. Lett. **41**, 264 (1978); Phys. Today **32** (8), 25 (1979).

⁵R. Meservey, P. M. Tedrow and V. R. Kalvey, Solid State Commun. **36**, 969 (1980).

⁶E. C. Stoner, Philos. Mag. **15**, 1018 (1933).

⁷C. S. Wang and A. J. Freeman, Phys. Rev. B **21**, 4585 (1980).

⁸O. Jepsen, J. Madsen, and O. K. Andersen, J. Magn. Mater. **15-18**, 867 (1980).

⁹H. Krakauer and A. J. Freeman, Bull. Am. Phys. Soc. **26**, 356 (1981).

¹⁰D. S. Wang, A. J. Freeman, and H. Krakauer, Phys. Rev. B **24**, 1126 (1981).

¹¹J. Noffke and L. Fritsche, J. Phys. C **14**, 89 (1981).

¹²E. W. Plummer and W. Eberhardt, Phys. Rev. B **20**, 1444 (1979).

¹³C. Rau and S. Iechner, Phys. Rev. Lett. **47**, 939 (1981).

¹⁴G. P. Felcher, S. D. Bader, R. J. Celotta, D. T. Pierce, and G. C. Wang, in *Ordering in Two Dimensions*, edited by S. K. Sinha (Elsevier, New York, 1980), p. 107.

¹⁵U. Gradmann, J. Appl. Phys. **40**, 1182 (1969).

¹⁶C. S. Wang and A. J. Freeman, Phys. Rev. B **24**, 4364

(1981).

¹⁷J. Tersoff and L. M. Falicov, Phys. Rev. B **25**, 4937 (1982).

¹⁸P. W. Anderson, Phys. Rev. **124**, 41 (1961).

¹⁹J. C. Slater and G. F. Koster, Phys. Rev. **94**, 1498 (1954).

²⁰*Handbook of Physico-chemical Properties of the Elements*, edited by G. V. Samsonov (Plenum, New York, 1968).

²¹C. Herring, *Exchange Interaction Among Itinerant Electrons*, Vol. IV of *Magnetism*, edited by G. T. Rado and H. Suhl (Academic, New York, 1966), and references therein.

²²H. Dannan, R. Heer, and A. J. P. Meyer, J. Appl. Phys. **39**, 669 (1968). The measured bulk magnetization of $0.616\mu_B$ is believed to reflect a spin imbalance $n_{\uparrow} - n_{\downarrow} = 0.56$ electrons per atom, with a *g* factor of 2.2 due to spin-orbit coupling; see Ref. 21.

²³C. S. Wang and A. J. Freeman, Phys. Rev. B **19**, 793 (1979).

²⁴L. M. Falicov and F. Yndurain, J. Phys. C **8**, 147 (1975); **8**, 1563 (1975).

²⁵S. L. Cunningham, Phys. Rev. B **10**, 4988 (1974).

²⁶J. Tersoff and L. M. Falicov, Phys. Rev. B **25**, 2959 (1982).

²⁷E. M. Gyorgy, J. F. Dillon, Jr., D. B. McWhan, L. W. Rupp, Jr., L. R. Testardi, and P. J. Flanders, Phys. Rev. Lett. **45**, 57 (1980).